J. Indian Inst. Sci., Sept.–Oct. 1997, 77, 421–437.

Performance characteristics of artificially commutated HVDC converter

V. R. KANETKAR, M. S. DAWANDE AND P. K. KALRA
Department of Electrical Engineering, Indian Institute of Technology, Kanpur (INDIA) 208016.

Abstract

Artificially commutated hvdc converter is analysed to obtain the steady state performance characteristics. These are presented in two parts. In part I, the converter is analysed for thyristor conduction overlap angle less than 60° to evaluate dv/dt, converter impedance and reactive power characteristics under constant output direct current and constant firing angle modes of operation. Non-characteristic harmonics in the ac line current arising due to firing imbalance are also presented.

In part II, the converter is analysed for thyristor conduction overlap angle greater than 60°. Operating characteristic reported include thyristor voltage, di/dt, dv/dt, ac/dc characteristic harmonics, converter impedances, effect of the line capacitive reactance on output dc voltage and power. These are presented to evaluate basic performance and constant output direct current mode of operation.

Comparison of the artificially commutated converter with naturally commutated converter is drawn at each stage to evaluate its suitability.

1. Introduction

Artificially Commutated Converter (ACC) has been analysed in the past to understand its potential application to hvdc transmission systems[1–4]. The basic operating characteristics like thyristor voltage, di/dt, output dc voltage and power have been reported earlier along with the possible extended firing angle range of 360°[1]. The harmonics in ac line current and output dc voltage,faults on ac side and converter responses have also been reported[2]. Further, power inversion to weak ac systems has been evaluated and reported[1–2]. A comparison of thyristor ratings for both Artificially Commutated Converter (ACC) and Naturally Commutated Converter (NCC) has been done along with the capacitor ratings[3]. Further, it has been shown that ACC can be used along with NCC to realise hybrid converter which has a feature of zero reactive power demand for given range of firing angle[4]. The ac line current and dc voltage harmonics of such a hybrid converter have been reported[4]. However, the ACC analysis in all the above papers is confined to overlap angle less than 60°.

In this paper the previously reported steady state ACC analysis is extended to cover the overlap angle range upto 120°. Comparison of ACC with NCC is drawn for the performance characteristic involving reactive power, dv/dt, converter impedance, harmonics in detail which have not been reported earlier in literature to the best of the knowledge of the authors.

2. Per unit system

The per unit system used remains same as reported in reference[1], i.e. the dc rated current and the ac line voltage have been chosen to be 1.0 p.u.

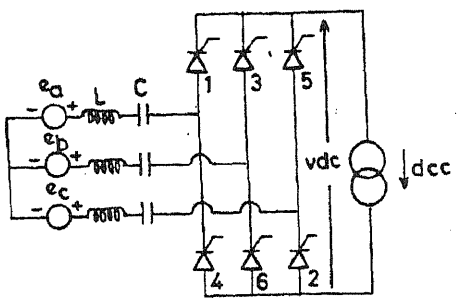

FIG. 1. Power circuit (ACC).

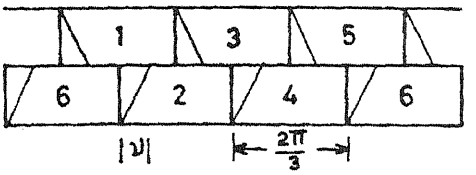

FIG. 2. Thyristor conduction ($\gamma < 60°$).

Power circuit and conduction modes

The power circuit considered for ACC is shown in fig. 1. The converter is modelled as a current source converter. The thyristor firing sequence is 1, 2, 3, 4, 5 and 6. The converter can operate in any of the following modes of conduction depending upon the angle of overlap (γ).

3. Angle of overlap (γ) less than 60°

The conduction pattern of the thyristors for this mode is shown in fig 2. It has three and two thyristors conducting alternately. Thyristor conduction period is ($120° + \gamma$) °. The commutation equivalent circuits are shown in fig. 3.

4. Angle of overlap (γ) greater than 60°

The conduction pattern of the thyristors for this mode is shown in fig. 4. It has four and three thyristors conducting alternately. Thyristor conduction period is $(120° + \gamma)°$. The commutaion equivalent circuits are shown in fig. 5.

The equivalent circuits shown in fig. 3 and 5 are used to derive, the commutation current, output direct current and voltage expressions. Commutation in both the circuits is assumed from thyristor 1 to 3.

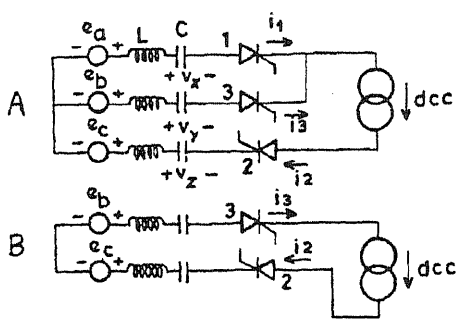

FIG. 3. Commutation equivalent circuits ($\gamma < 60°$).

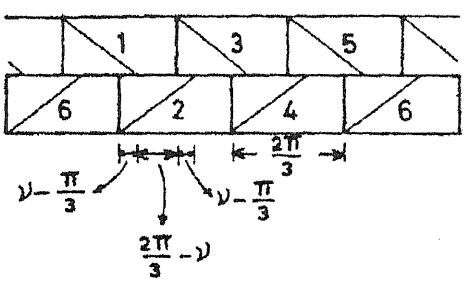

FIG. 4. Thyristor conduction ($\gamma > 60°$).

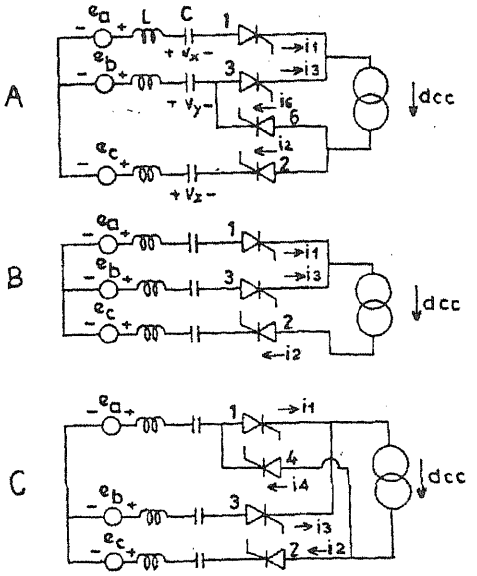

FIG. 5. Commutation equivalent circuits ($\gamma > 60°$).

The commutation current(s) as well as the output dc voltage expressions given in[1] appear to have typographical errors. Also, no expression for output direct current is explicitly given in any of the reported papers. As such, for the ready reference of the user, simplified expressions for output direct current and voltage are given in appendix-I. Corresponding expressions for overlap angle greater than 60°, along with the necessary explanations towards their derivations, are presented in appendix-II. For obtaining expressions, the following three phase voltage are assumed.

$$e_a = v_{pm} \sin(\omega t + \alpha + 150°)$$
$$e_b = v_{pm} \sin(\omega t + \alpha + 30°)$$
$$e_c = v_{pm} \sin(\omega t + \alpha - 90°)$$

Further the thyristor 3 is fired at $\omega t = 0.0°$ to commutate thyristor 1.

PART- I : STEADY STATE PERFORMANCE (OVERLAP ANGLE LESS THAN 60°)

The control modes considered are given below:

A. Constant output direct current

The independent variable considered for this mode is firing angle.

B. Constant firing angle

The independent variable considered for this mode is output direct current. Constant output direct current mode is a commonly used mode for hvdc converters. The constant firing angle

characteristics obtained from the output direct current and voltage expressions given in appendix-I can be effectively used to accommodate the constant extinction angle characteristics. These are of concern for inverter operation[5]. As such, the modes A and B together are adequate to understand the ACC operation.

Further, to understand the behaviour of ACC in these modes, active and reactive power characteristics are derived using the output direct current and voltage expressions (appendix-I) and using the ac line current model suggested in references[2]. These characteristics give an indication of how the capacitive reactance influences the reactive power and hence, the power factor of operation.

dv/dt stress on the thyristors is an important parameter for selection of these devices and the associated damper circuits. This is analysed in both modes A and B.

When the converter forms a part of the total transmission network, it becomes necessary to model it as a variable impedance presented to the ac bus. NCC has been already modelled to this effect and presented[6]. The impedance is normally consisting of a parallel combination of resistance and reactance connected to the ac bus.

These elements are functions of the firing angle as well as the overlap angle. In a similar way, when the converter draws power from a dc source, it needs to be represented as a resistive impedance connected across the dc source. A study has been done to determine the variation of these impedance's under both modes A and B. This will facilitate modelling the converter as a variable ac/dc impedance for stability and voltage collapse studies.

Non-characteristic harmonics in ac line current are generated due to supply unbalance or due to the thyristor firing imbalance and they have an impact on the input ac line filter and transformer design. The firing imbalance is more likely to exist during normal operation[7]. The study of these non-characteristic harmonics is restricted here to only firing imbalance which is considered to be $C = 2°$. Firing of thyristor 1, 3, 5, is advanced and that of thyristors 4, 6, 2 is retarded by $C = 0°$. Further, the total conduction period of thyristor 1 and 4 is reduced by C°. The ac line current model remains same as suggested in reference[2].

Observation (ACC w. r. t. NCC)

1. Active power, reactive power and dv/dt characteristics for modes A and B are given in fig. 6 and 7. The range for mode A is restricted upto 145° since this is where the NCC operation stops. However, it must be noted that the ACC characteristics are extendable beyond this. In mode B the characteristics are compared upto output direct current value of 1.2 p.u.

   The active power characteristics in both modes A and B show a small increase in power with the ACC. In mode A, these characteristics exhibit different slopes in three regions namely 0–60°, 60°–120° and 120°–145°. In mode B, the characteristics are practically the same for ACC and NCC upto direct current value of 0.7. However, beyond this value of 0.7, the ACC characteristics changes its slope and shows increase in power. The reactive power with ACC is smaller compared to NCC upto $\alpha = 120°$ in mode A. The difference increase towards $\alpha = 0°$ where the reactive power drops to almost 20% compared to that of NCC (characteristic with $Xc = 0.9$). Beyond $\alpha = 120°$ the NCC reactive power starts dropping at a

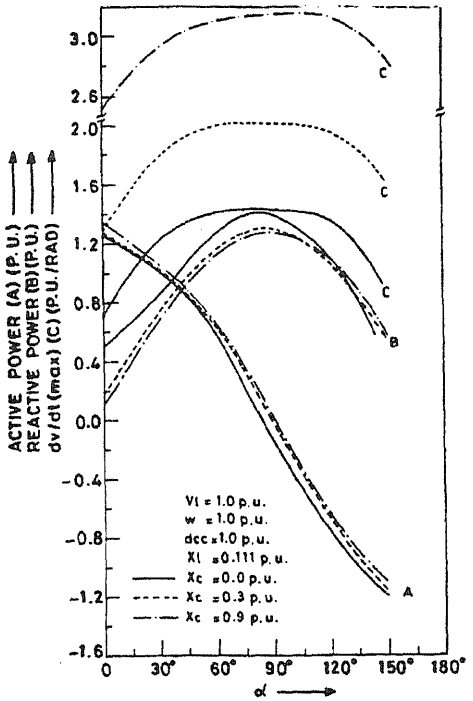

FIG. 6. Active power, reactive power and dv/dt variation for control mode A ($\gamma < 60°$).

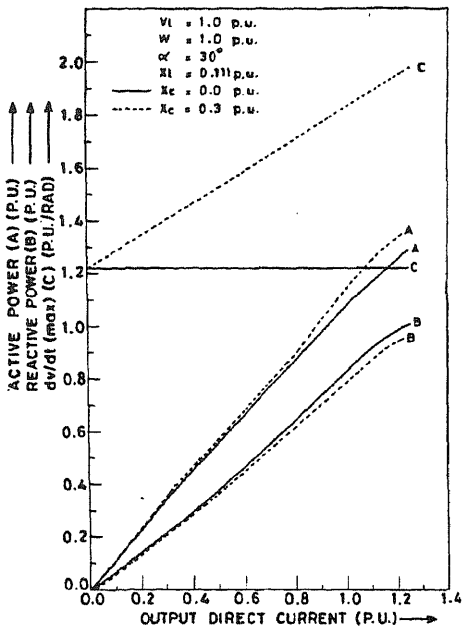

FIG. 7. Active power, reactive power and dv/dt variation for control mode B ($\gamma < 60°$).

faster rate as compared to ACC. Beyond $\alpha = 135°$ it is smaller than ACC. In mode B, the characteristics are practically the same for ACC and NCC upto output direct current value of 0.7. However, beyond this value of 0.7, the ACC characteristics changes its slope and shows a decrease in reactive power.

The dv/dt characteristics in both modes A and B show a marked difference. In mode A, the characteristics are similar to bath-tub curves. In mode b, the dv/dt characteristics for NCC is a constant value characteristics and for ACC it varies linearly with the output direct current. It shows clearly that in both modes the dv/dt faced by the thyristors increases considerably with the ACC. The maximum values observed are compared in Table I. The increase in dv/dt is a point of concern for ACC designs.

Table I

dv/dt (max) p.u./rad observed for $\gamma < 60°$. Bracketted figures give the percentage increase for ACC over the corresponding NCC values.

	NCC	ACC		REMARKS	
	Xc°= 0.0	Xc°= 0.3	Xc°= 0.9	dcc°= 1.0,	X1°= 0.111
Mode A	1.414	1.933(41)	3.155(123)	α = 30°,	X1°= 0.111
Mode B	1.225	1.961(60)		α = 30°,	X1°= 0.111

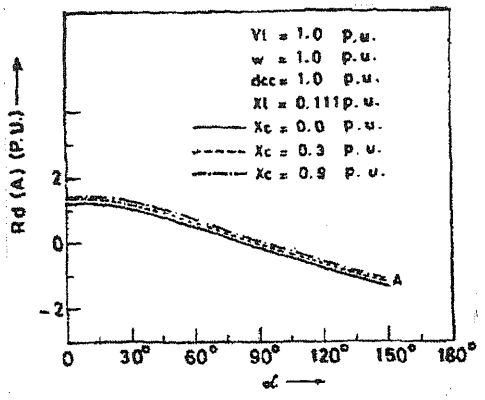

FIG. 8. Onput dc resistance variation for control mode A ($\gamma < 60°$).

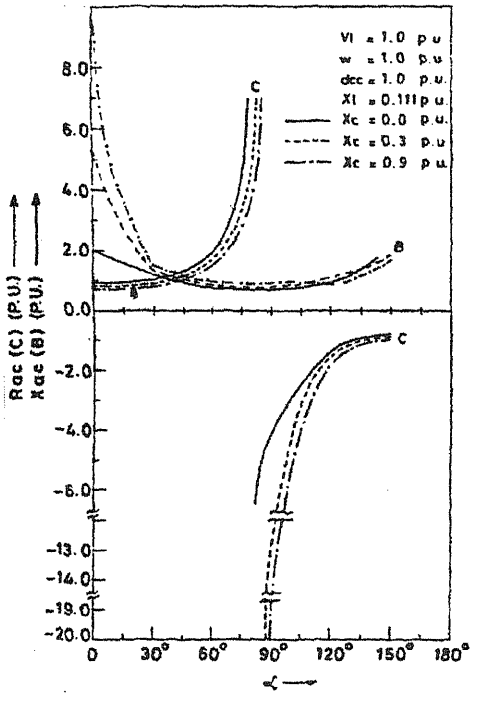

FIG. 9. Input shunt resistance and reactance variation for control mode A ($\gamma < 60°$).

2. Converter impedances (output resistance Rd, input shunt resistance Rac and reactance Xac) variations for mode A are shown in fig. 8 and 9 and for mode B are shown in fig. 10. These characteristics reflect the active and reactive power behaviours of the converters.

   The converter output resistance Rd depends upon the ratio active power/(output direct current)^2. In mode A, since the output direct current is constant the output resistance Rd is proportional to active power. This can be seen from the characteristics in fig. 8. In mode B, the output direct current varies and since the active power characteristic is linear, the output resistance characteristic is inversely proportional to the output direct current (fig. 10). The ACC and NCC output resistance characteristic are, however, close to each other.

The reflected shunt resistance Rac and reactance Xac vary inversely in proportion to the active power and reactive power demand of the converter. As the powers tend to zero these impedances increase rapidly. This is clear from the figs. 9 and 10.

The non-characteristic harmonics have been analysed only for most relevant case, i.e. imbalance in thyristor firings. These are plotted for mode B since it gives an idea of the entire output direct current range operation (fig. 11). The imbalance effect in terms of these non-characteristics harmonics can be summarised as below :

(a) All these non-characteristic harmonics for ACC as well as NCC are less than 3% value of the operating direct current.

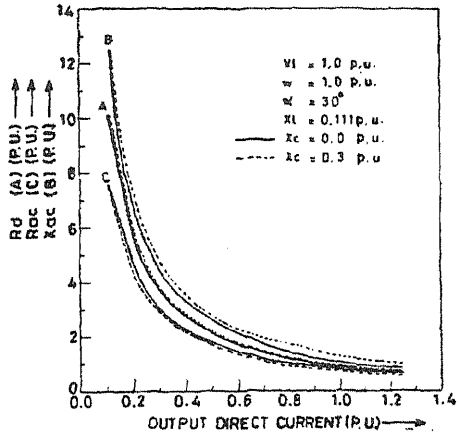

FIG. 10. Output dc resistance, input shunt resistance and reactance variation for control mode B ($\gamma < 60°$).

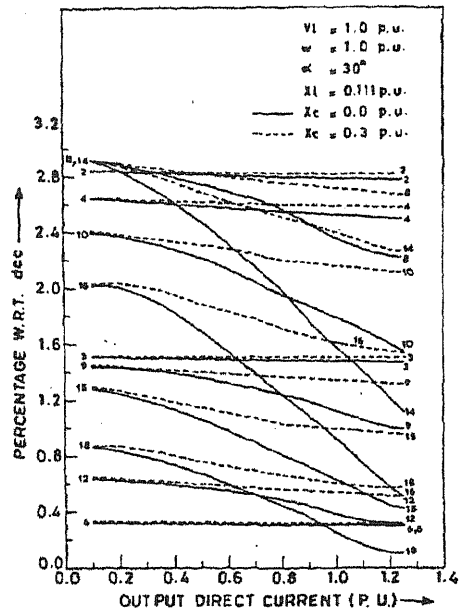

FIG. 11. Non-characteristic harmonics (ac line current) for control mode B ($\gamma < 60°$).

(b) As the harmonic number increases, its percentage reduces.

(c) Harmonic 2, 3, 4, and 6 show almost the same value in both ACC as well as in NCC.

(d) Beyond 6th harmonic, the percentage of harmonics in ACC increases w.r.t. those in NCC. Typical comparison at output direct current of 1.00 p.u. shows that in ACC the 8th harmonic increases by 15% and 18th harmonic increases by 150% over the corresponding values of 8th and 18th harmonic of NCC. The harmonic between 8th and 18th show the percentage increase between 15 to 150. It should be noted that the absolute percentage values are however small. Considering that the percentage is less than 3% for all the harmonics, a single high-pass filter could be used effectively to attenuate higher order harmonics beyond 6. The lower order harmonics below 6, if necessary, could be attenuated with tuned filters.

Part II: Steady state performance (overlap angle greater than 60°)

Like NCC this mode in ACC is characterised by high current and low voltage operation. The line capacitive reactance, however, controls the output current. Fig. 12 shows typical output dc voltage vs current characteristics for ACC as well as NCC operating in this mode. Operating region for NCC is between $\alpha = 30°$ to 90° while for ACC is observed between $\alpha = 210°$ to 270°. The output dc voltage and power decrease as the capacitive reactance is increased. This effect is shown in fig.13. The analysis of ACC with this mode of overlap angle is presented in two parts as below:

a) Basic Performance

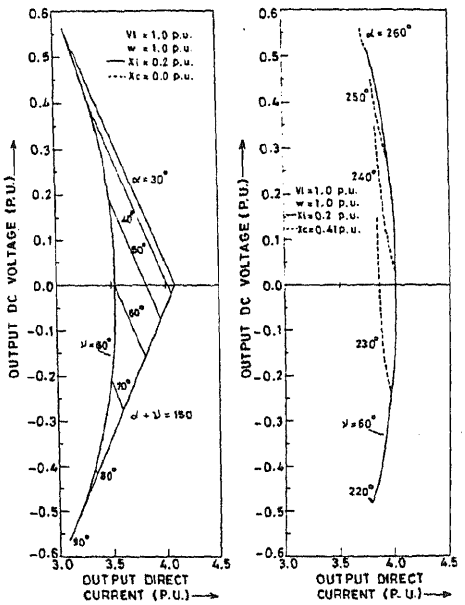

FIG. 12. Output dc voltage vs output direct current characteristics ($\gamma > 60°$).

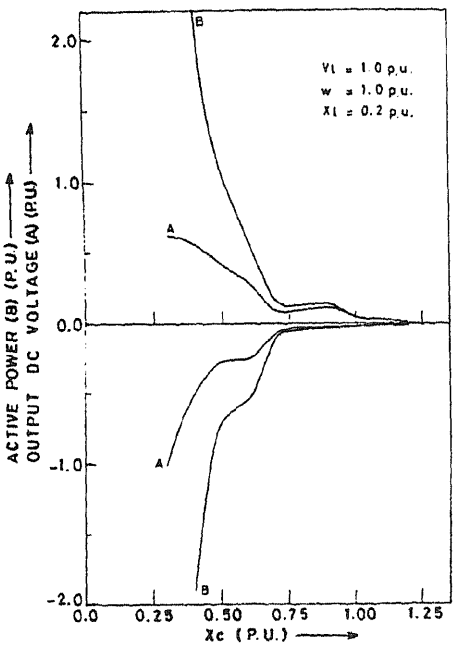

FIG. 13. Output dc voltage vs capacitive reactance and output power vs capacitive reactance characteristics ($\gamma > 60°$).

b) Constant output direct current control mode (control mode A).

Basic performance for ACC is compared with NCC at the same operating point. The operating point chosen has same values output direct current, voltage and hence, the output power. The operating characteristics compared include commutation current, di/dt, thyristor voltage, dv/dt and characteristic harmonics in ac line current and output dc voltage. These are given in figs. 14 to 18. The constant output direct current control mode (control mode A) is chosen on the similar lines as the mode A examined under overlap angle less than 60° operation. The output direct current is constrained here between 3.5 to 3.7 p.u. (average value 3.6 p.u.). The performance of ACC and NCC is then analysed throughout the corresponding available firing range. For the set of values chosen ($xl = 0.2$, $xc = 0.43$), it is found that the NCC firing angle range between 30° to 70° and ACC firing angle range between 230° to 260° gives approximately the same output power range (–0.86 to 1.75 p.u.). As such, instead of the firing angle, output power is chosen as the independent variable to plot the performance characteristics. The performance characteristics include di/dt, thyristor voltage, dv/dt, reactive power, converter impedances and characteristic harmonics in ac line current and output dc voltage. These are given in figs. 21 to 27.

The ac line current waveform considered for analysis is given in fig. 19. A typical waveform of the line capacitor voltage is shown in fig. 20. The output dc voltage consists of 6 pulses/cycle. The pulse shape is as given in fig. 15.

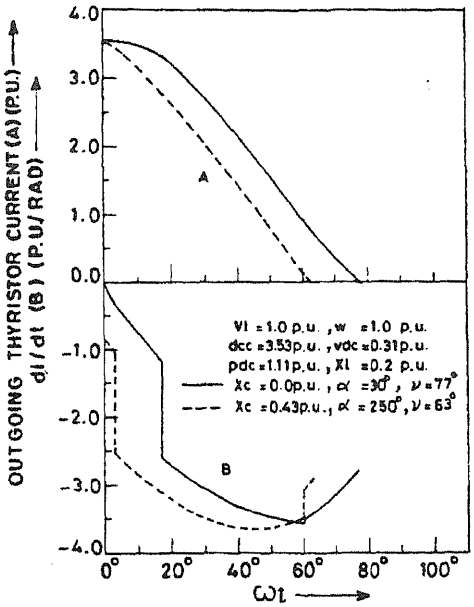

FIG. 14. Commutation current and di/dt characteristics ($\gamma > 60°$).

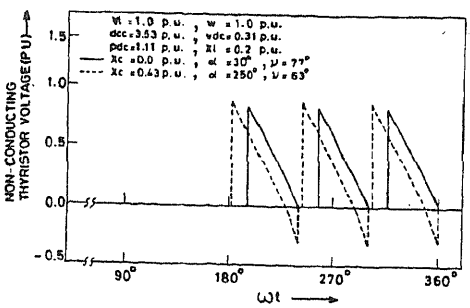

FIG. 15. Thyristor voltage variation ($\gamma > 60°$).

Observations (ACC w.r.t. NCC)

1. For the same operating point (output direct current and voltage), the commutation overlap angle reduces for ACC. As a consequence, the initial di/dt value is higher in ACC (fig.14). However, the di/dt (max) is of the same order (3.55 p.u./rad for ACC against 3.5 p.u./rad for NCC). This is observable from fig. 14 for same operating point as well as fig. 24 for control mode A.

2. The maximum thyristor voltage and dv/dt (max) also do not change appreciably in ACC as compared to NCC. This is possible to conclude from figs. 15 and 16 for same operating point as well as from figs. 24 and 25 for control mode A. However, as shown in fig. 25 for control mode A, the thyristor voltage decreases by almost 33% in ACC compared to NCC when active power demanded becomes zero.

3. ACC draws leading reactive power. The characteristic is observed to be flat in the major operating range (active power variation between -0.8 to 1.0 p.u.) for control mode A. The NCC and ACC characteristics appear to be mirror image of each other (fig. 21.).

4. The converter impedance characteristics (output resistance Rd and input shunt resistance Rac) closely match for ACC and NCC in control mode A (figs 22 and 23). Since the output current is constant, the output resistance (Rd) varies linearly with output power. The input shunt resistance (Rac), however, varies inversely with the active power. The input shunt reactance (Xac) also varies inversely with the reactive power. Since the reactive power in control mode A has a flat characteristic, the same is exhibited by the input shunt reactance

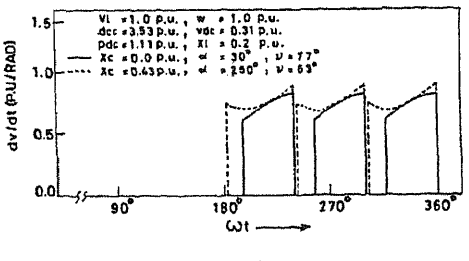

FIG. 16. dv/dt variation ($\gamma > 60°$).

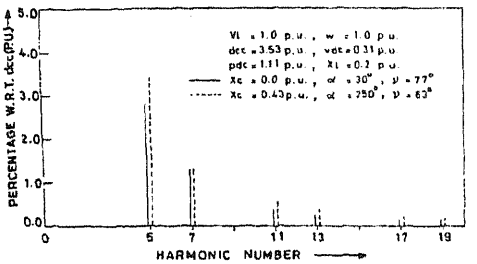

FIG. 17. Characteristic harmonics (ac line current) ($\gamma > 60°$).

(Xac) characteristics (fig. 22).The characteristics of NCC and ACC also remain mirror image of each other.

5. For the same operating point, characteristic harmonics in ac line current and output dc voltage appear to be higher in ACC as compared to NCC (figs. 17 and 18). However, when the entire power range as in control mode A is considered (figs. 26 and 27) it shows that:

   e) the 7, 11 & 13th harmonics in ac line current for ACC remain of the same order as those for NCC. The 5th harmonic, on the other hand, is more in ACC in two regions (active power region between -0.86 to 0.38 and 0.35 to 1.5 p.u.). The maximum differential in-

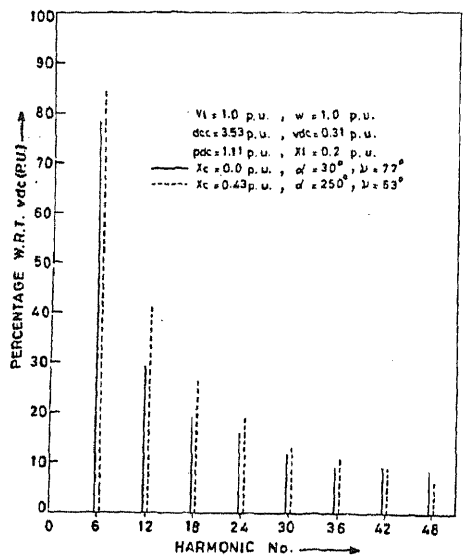

FIG. 18. Characteristic harmonics (output dc voltage ($\gamma > 60°$).

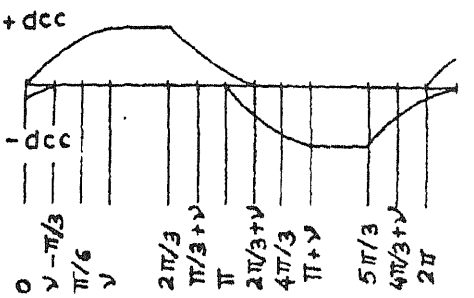

FIG. 19. AC line current waveform ($\gamma > 60°$).

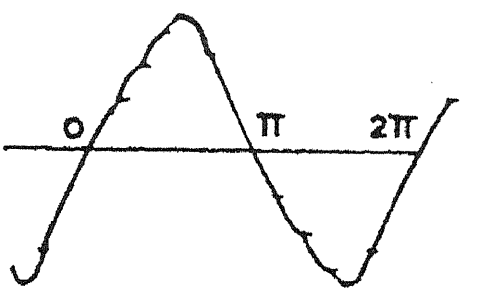

FIG. 20. Capacitor voltage waveform ($\gamma > 60°$).

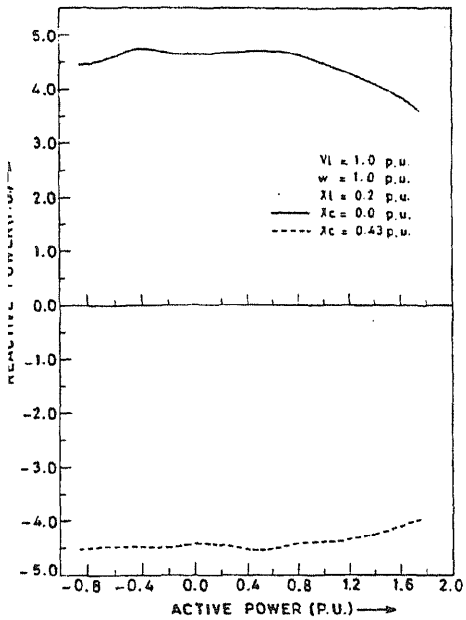

FIG. 21. Reactive power vs active power characteristics ($\lambda > 60°$).

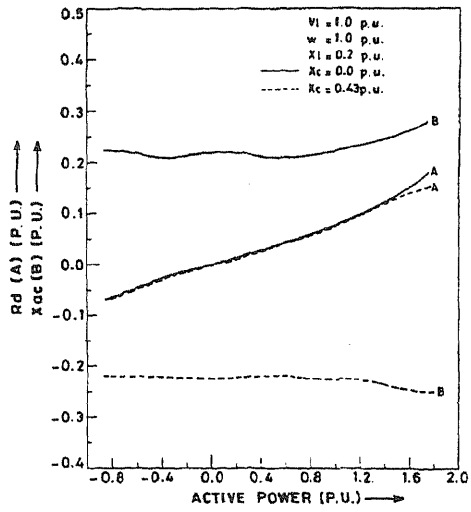

FIG. 22. Output dc resistance vs active power and input shunt reactance vs active power variation ($\lambda > 60°$).

crease in the 5th harmonic for ACC is only 0.67% observed at 0.8 p.u. active power. As the active power demanded reduces to zero, the 5th harmonic in ACC falls down substantially. However, in both ACC as well as in NCC the harmonics in ac line current are less than 4%.

f) the dc voltage harmonics do not vary substantially in ACC and NCC except in the region 0 to -0.4 p.u. of active power. In this region the ACC harmonic percentage falls down as compared to that of NCC. Overall the harmonics are below 0.35 p.u. absolute value.

5. Considering that the output power can be substantially reduced by increasing the capacitive reactance in line (fig. 13) and the ac line current harmonics are small (fig. 26), the ACC in this overlap mode angle of greater than 60° shows possibility of its use as a reactive power controller.

7. The operating range of the firing angle for ACC is restricted from 210° to 270° as against the range of 30° to 90° for NCC. The output power range (as in control mode A) can be maintained same for both ACC and NCC (fig. 12). It is observed that Xc/X1 ratio around 2.15 gives this range. This ratio also gives the power inversion capability for ACC into a weak ac system over the entire output power range.

Conclusions

Overlap angle less than 60°

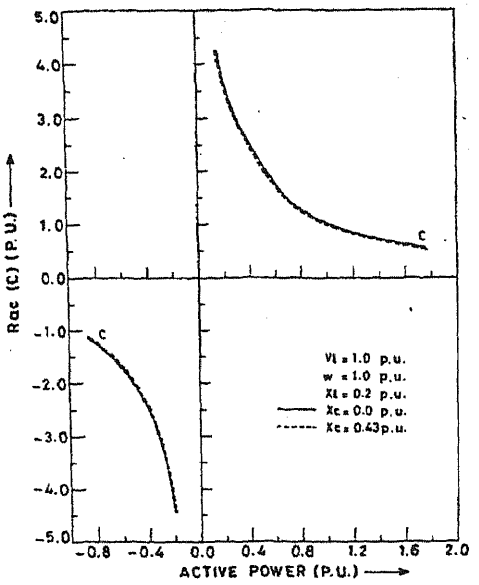

FIG. 23. Input shunt resistance vs active power variation ($\gamma > 60°$).

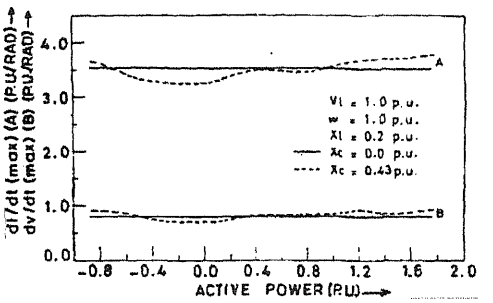

FIG. 24. di/dt (max) vs active power and dv/dt (max) vs active power variation ($\gamma > 60°$).

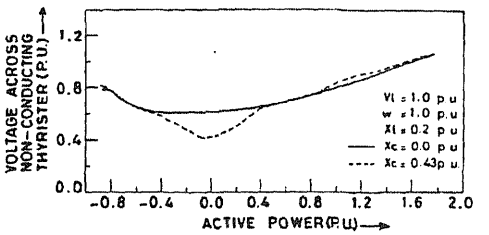

FIG. 25. Thyristor voltage vs active power variation ($\gamma > 60°$).

The reactive power drawn by ACC can be reduced in comparison with NCC over maximum possible operating range of the firing angle by properly selecting the Xc/X1 ratio. However, the dv/dt stress on the thyristors increases considerably as this ratio increases. This can have constraints on the ACC design and implementation. The non-characteristic harmonics in ac line are observed to be less than 3% of the operating output direct current. This is for a firing imbalance of 2°. Thus, they do not pose any serious threat to the input filter design. A single highpass filter can be effectively used to attenuate the higher order harmonics beyond 6 to an acceptable limit. The lower order harmonics, if necessary, could be attenuated with tuned filters. Converter impedance characteristics presented give an insite for the ACC to be modelled as a variable impedance connected to an ac or dc terminals. This will be useful for stability studies.

Overlap angle greater than 60°

This mode is adequately analysed to understand basic performance of ACC. To obtain the same output power range as that of NCC, Xc/X1 ratio around 2.15 can be used a guideline value. Increase in the capacitive reactance (Xc), however decreases the output power range. It is shown that the thyristor voltage, di/dt and dv/dt stresses on the thyristors are comparable to those observed with NCC. The characteristic harmonics in ac line are below 4% of the operating output direct current value both for ACC and NCC. The harmonics are comparable, except 5th, which decreases considerably in ACC as the active power reduces to zero. The characteristic harmonics in output dc voltage of ACC do not vary substantially except in the region 0 to -0.4 p.u. of the active power where the ACC shows drop in the harmonic percent-

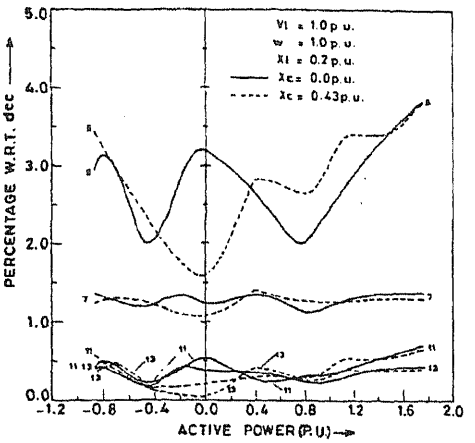

FIG. 26. Characteristic harmonics (ac line current) vs active power variation ($\gamma > 60°$).

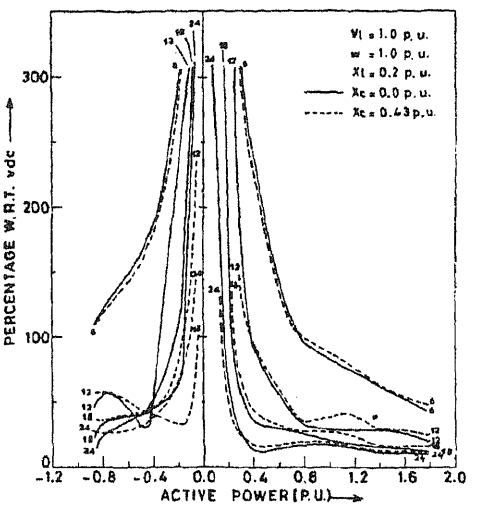

FIG. 27. Characteristic harmonic (output dc voltage) vs active power variation ($\gamma > 60°$).

ages. Overall the harmonics are below 0.35 p.u. absolute value. The ACC draws leading reactive power in this overlap mode. The active power can be considerably reduced by increasing the Xc/X1 ratio. Since, the ac line current harmonics are small, ACC in this overlap angle mode of operation shows its possible application as a reactive power controller. This aspect needs to be examined in detail. Converter impedance characteristics presented can be effectively used for modelling the converter as a variable impedance connected to an ac or dc bus for stability studies.

APPENDIX I

$$\text{dcc} = \frac{\left[\dfrac{\sqrt{3}\omega v_{pm}}{2L(\omega^2-\omega_n^2)}\left[\cos(\alpha+\gamma)-E5\cos\alpha+\dfrac{D5}{1+E5}\left[-D5\cos\alpha+\dfrac{\omega_n}{\omega}\sin\alpha+\dfrac{\omega_n}{\omega}\sin(\alpha+\gamma)\right]\right]\right]}{\left[-1+\dfrac{(4\pi-3\gamma)\dfrac{\omega_n}{\omega}D5}{6(1+E5)}\right]}$$

$$\text{vdc} = \frac{3\sqrt{3}V_{pm}}{2\pi}\left[\cos\alpha+\cos(\alpha+\gamma)\right]$$

$$+\frac{3\sqrt{3}V_{pm}}{2\pi}\left[\frac{\omega_n^2}{\omega^w-\omega_n^2}\right]\left[\frac{\dfrac{2\pi}{3}-\dfrac{\gamma}{2}}{1+E5}\right]\left[\sin(\alpha+\beta)-E5\sin\alpha-\frac{\omega}{\omega_n}D5\cos\alpha\right]$$

$$+\frac{dcc}{\pi C\omega(1+E5)}\left[\left(2\pi\gamma-\frac{3\gamma^2}{4}-\frac{4\pi^2}{3}\right)(1-E5)+\frac{\omega}{\omega_n}\left(2\pi-\frac{3\gamma}{2}\right)D5\right]$$

Constants used in the above expressions are given at the end of Appendix-II.

APPENDIX II

From the thyristor conduction pattern given in Fig. 3 and the equivalent circuits given in Fig. 5. It can be seen that thyristor current i1 decreases to zero and the thyristor current i3 increases to doc in the overlap durtion of γ^0. Considering this, the current I1 has the following governing equations obtained from the three modes A, B, C given in Fig. 5.

Mode	Equations	Initial Conditions
A	$e_a - L\frac{di1}{dt} - v_x = 0$	i1(0) = dcc, $v_x(0)=V_{x1}$, $v_y(0)=V_{y1}$, $v_z(0)=V_{z1}$
B	$e_b - e_a + 2L\frac{di1}{dt} + v_x - v_y = 0$	i1(0) = i1(2), $v_x(0)=V_{x2}$, $v_y(0)=V_{y2}$, $v_z(0)=V_{z2}$
C	$e_b + L\frac{di1}{dt} - v_y = 0$	i1(0) = i1(3), vx(0)=Vx3, vy(0)=Vy3, vz(0)=Vz3

Considering the 60° symmetry of the circuit

$$V_{y3} = -V_{z1} = V_{x1} + V_{y1} \text{ as } V_x + V_y + V_z = 0$$

Thus, to evaluate i1 in all modes following six variables will have to be calculated.

$$V_{x1}, V_{y1}, V_{x2}, V_{y2}, i1(2) \text{ and } i1(3)$$

These require six simultaneous equations to evaluate them. The required equations can be obtained in various ways. One of the ways is as suggested below.

Obtain four equations based on charging of the capacitors in phase 'a' and phase 'b' in modes A and B. These equations are related to V_{x1}, V_{x2}, V_{y1} and V_{y2}. i1(2) and i1(3) are end conditions of mode A and B respectively. Hence, these yield two equations related to i1(2) and i1(3).

After solving for these six variables, i1 can be equated to zero at t = γ/ω to get the dcc expression.

Because of the 60° symmetry, the average dc voltage (vdc) can be obtained by considering average over a period of 60°. Consider the modes A and B of Fig. 5.

In mode A, four thyristors conduct and hence, the output voltage is zero for duration (γ-60)°.

In mode B, the instantaneous dc voltage vdc (ωt) is given by

$$v_z - v_x + e_a - e_c - L\frac{di1}{dt}$$

The commutation loop equation is

$$v_x - v_y + e_b - e_a + 2L\frac{di1}{dt} = 0 \text{ as } i1 + i3 = dcc$$

Using the loop equation, vdc (ωt) can be rewritten as below.

$$vdc(\omega t) = \frac{3}{2}(v_z - e_c)$$

Therefore, average dc voltage vdc will be

$$\text{vdc} = \frac{3}{\pi}\int_0^{(120-\gamma)^o} \frac{3}{2}(v_z - e_c)d\omega t$$

However, to evaluate this expression initial voltage v_{z2} is required. In mode BB, the capacitor voltage v_z changes from v_{z2} to v_{z3} or V_{z2} to $-V_{x1}$ (using the 60^0 symmetry).

Therefore, $V_{z2} = \frac{dcc}{C\omega}(2\pi/3 - \gamma) - V_{x1}$ where V_{x1} where V_{x1} is already known. Thus, the average dc voltage vdc can be obtained.

The dcc and vdc expression based on above procedures are as given below.

$$dcc = \frac{Num}{Den}$$

$$Num = \frac{V_{pm}\omega}{L(\omega^2 - \omega_n^2)}\left[\left(\frac{E3}{2} - E5\right)\sin(\alpha + 60) + \cos(\alpha + \gamma + 30) + \frac{E6}{2}\sin(\alpha + \gamma - 60)\right.$$

$$\left. + \frac{\omega_n}{\omega}\left[\left(\frac{D3}{2} - D5\right)\cos(\alpha + 60) + \frac{D6}{2}\cos(\alpha + \gamma - 60)\right]\right.$$

$$\left. + \frac{\left(\frac{D3}{2} + \frac{D6}{2} - D5\right)}{(E6 - 2E5 + E3 - 2)}\left[(D3 - 2D5)\sin(\alpha + 60) + D6\sin(\alpha + \gamma - 60)\right.\right.$$

$$\left.\left. + \frac{\omega_n}{\omega}(2E5 - E3)\cos(\alpha + 60) + \frac{\omega_n(2 - E6)\cos(\alpha + \gamma - 60)}{\omega}\right]\right]$$

$$Den = \left[\frac{\omega_n}{2\omega}D6\left(\frac{2\pi}{3} - \gamma\right) + \frac{1}{2}(E6 - 2E5 + E3 - 2)\right.$$

$$\left. + \frac{1}{(E6 - 2E5 + E3 - 2)}\left[\frac{\omega_n}{\omega}(2 - E6)\left(\frac{2\pi}{3} - \gamma\right)\left(\frac{D3}{2} + \frac{D6}{2} - D5\right) + 2\left(\frac{D3}{2} + \frac{D6}{2} - D5\right)^2\right]\right]$$

$$vdc = \frac{9V_{pm}}{2\pi}\left[\cos(\alpha-30)+\cos(\alpha+\gamma+30)\right]+\frac{9}{4\pi}\frac{dcc}{\omega C}\left(\frac{2\pi}{3}-\gamma\right)^2$$

$$-\frac{9(2\pi/3-\gamma)}{2\pi\omega_n C(E6-2E5+E3-2)}\left[\frac{V_{pm}\omega}{L\left(\omega^2-\omega_n^2\right)}\left\{\frac{\omega_n}{\omega}\left[(2E5-E3)\cos(\alpha+60)\right.\right.\right.$$

$$\left.+(2-E6)\cos(\alpha+\gamma-60)\right]+(D3-2D5)\sin(\alpha+60)$$

$$\left.\left.+\ D6\sin(\alpha+\gamma-60)\right\}\right.$$

$$\left.+\ \text{dcc}\left[\frac{\omega_n}{\omega}\left(\frac{2\pi}{3}-\gamma\right)(E6-2)-D6-D3+2D5\right]\right]$$

The constants used in the above expressions are

D3	= $\sin[(\omega_n/\omega)(\gamma-\pi/3)]$	,	E3	=	$\cos[(\omega_n/\omega)(\gamma-\pi/3)]$
D4	= $\sin[(\omega_n/\omega)(2\pi/3-\gamma)]$	,	E4	=	$\cos[(\omega_n/\omega)(2\pi/3-\gamma)]$
D5	= $\sin[(\omega_n\gamma/\omega)]$	,	E5	=	$\cos[(\omega_n\gamma/\omega)]$
D6	= $\sin[(\omega_n\pi/3\omega)]$	,	E6	=	$\cos[(\omega_n\pi/3\omega)]$

NOMENCLATURE

C	=	Commutation capacitance
dcc	=	Output direct current
i1	=	Outgoing thyristor current (thyristor 1 considered)
L	=	Commutation inductance
Rd	=	Output dc resistance
Rac	=	Reflected ac shunt resistance/phase
t	=	real time
vdc	=	Output dc voltage
V1	=	Line voltage
V_{pm}	=	Phase voltage peak
v_x	=	Instantaneous voltage of capacitor in phase 'a'
v_y	=	Instantaneous voltage of capacitor in phase 'b'
v_z	=	Instantaneous voltage of capacitor in phase 'c'
ω	=	Supply angular frequency (rad/s)
ω_n	=	Natural frequency in commutation loop (rad/s)
Xac	=	Reflected ac shunt reactance/phase
Xc	=	Capacitive reactance in line (ωC)
X1	=	Commutation reactance (ωL)
α	=	Firing angle of the thyristors
γ	=	Commutation overlap angle

References

1. REEVE, J., BARON, J. A. AND HANELY, G. A., A technical assessment of artificial commutation of hvdc converters with series capacitors, *IEEE Trans. On Power Apparatus and Systems*, Vol. PAS-87, **10**, 1968, pp. 1830–1840.
2. GOLE, A. M. AND MENZIES, R. W. Analysis of certain aspects of forced commutated hvdc inverters, *IEEE Trans. on Power Apparatus and Systems*, Vol. PAS-100, **5**, 1981, pp. 2258–2262.
3. KWA-SUR TAM AND LASSETER, R., Implementation of the hybrid inverter for hvdc/weak ac system interconnection, *IEEE Trans. on Power Delivery*, Vol. PWRD-1, **4**, 1986, pp. 259–267.
4. KWA-SUR TAM AND LASSETER, R., A hybrid converter for hvdc application, *IEEE trans. on Power Electronics*, Vol. PE-2, **4**, 1987, pp. 313–319.
5. KIMBARK, E. W., Direct current transmission. New York : Wiley Interscience, 1971, Chapter 4.
6. WATSON, D. B. Circuit representation of three -phase bridge converters, *Int. J. Elect. Engg. Educ.*, Vol. 25, 1988, pp. 351–360.
7. REEVE, J. AND KRISHNAYYA, P.C. S., Unusual current harmonics arising from high-voltage dc transmission, *IEEE Trans. on Power Apparatus and Systems*, Vol. PAS-87, **3**, 1968, pp. 883–893.

V.R. KANETKAR received the B.E. (Electrical) degree in 1976 from Walchand College of Engineering (Shivaji University) Sangali and M.Tech (Electrical) degree in 1978 from IIT Bombay. From 1978 to 1989 he worked with M/S Larsen and Turbo Ltd., Bombay in their R & D for development of dc drives, slip ring motor controls and equipments for harsh environments. His research interested include electrical drives, power electronics and HVDC. He is presently working for his Ph.D. degree at IIT Kanpur.

MRS. M.S. DAWANDE received the B.E. (Electrical) degree in 1983 from Govt.Engineering College, Amravati and Master's degree in 1990 form Nagpur University. She has been a Lecturer in Electrical Engineering from 1983 and is associated with R.K.N.E. College, Nagpur. Her research interest Power electronics and microprocessor applications. She is presently working for her Ph.D. degree at IIT Kanpur.

PREM KUMAR KALRA, (M'87) was born in Dayalbagh, Agra on October 25, 1956. He received the B.Sc., M.Tech. and Ph.D. degrees, all in electrical engineering in 1978, 1982 and 1987, respectively. He is presently an Professor at the Indian Institute of Technology, Kanpur, India. His research interests include HVDC, power electronics, power system control and expert systems.